CHEMISTRY
A EUROPEAN JOURNAL

Supporting Information

Structure, Magnetism and Theory of a Family of Nonanuclear $Cu^{II}_5Ln^{III}_4$– Triethanolamine Clusters Displaying Single-Molecule Magnet Behaviour

Stuart K. Langley,[a] Liviu Ungur,[b] Nicholas F. Chilton,[a] Boujemaa Moubaraki,[a] Liviu F. Chibotaru,[b] and Keith S. Murray*[a]

chem_201100218_sm_miscellaneous_information.pdf

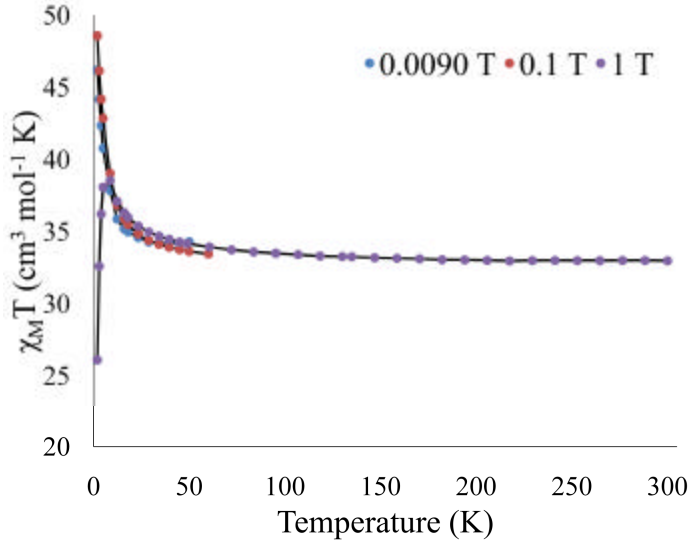

Figure S1. $?_M T$ versus T plot for **1** in DC fields of 1 T (2 – 300 K), 0.1 T and 0.01 T (2 – 70 K).

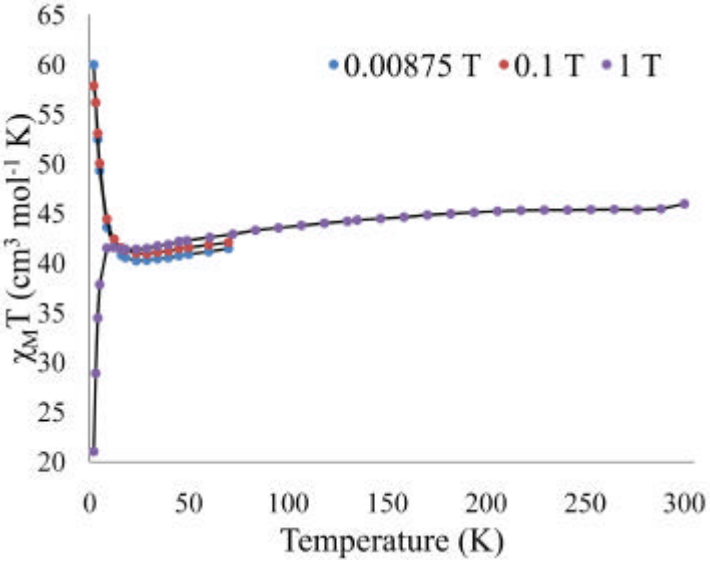

Figure S2. $?_M T$ versus T plot for **2** in DC fields of 1 T (2 – 300 K), 0.1 T and 0.01 T (2 – 70 K).

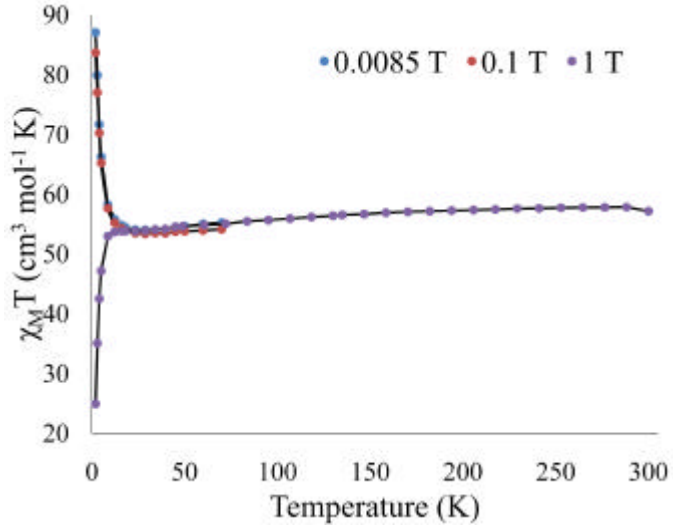

Figure S3. ?$_M$*T* versus *T* plot for **3** in DC fields of 1 T (2 – 300 K), 0.1 T and 0.01 T (2 – 70 K).

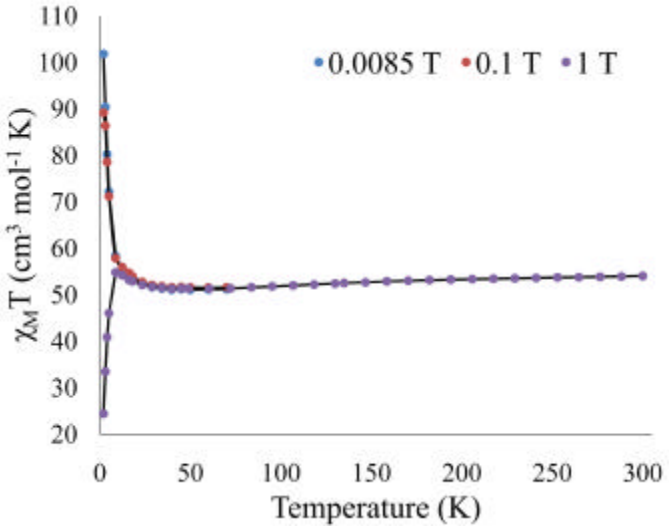

Figure S4. ?$_M$*T* versus *T* plot for **4** in DC fields of 1 T (2 – 300 K), 0.1 T and 0.01 T (2 – 70 K).

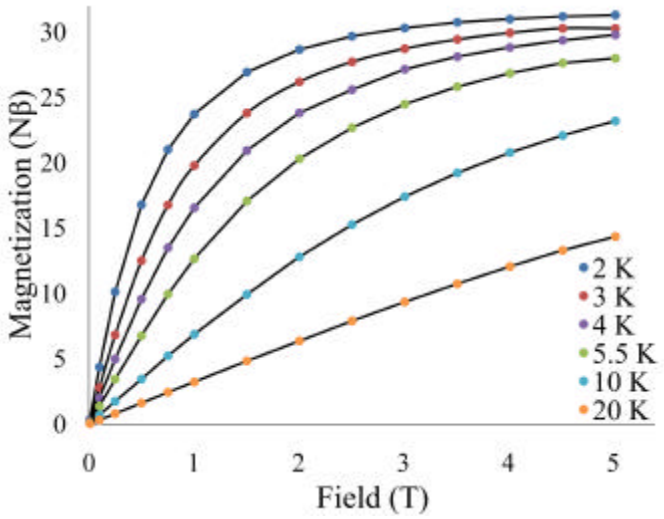

Figure S5. *M* vs *H* isothermal plots for **1** in the 2 (top) – 20 K (bottom) temperature range. The solid lines are guides for the eye.

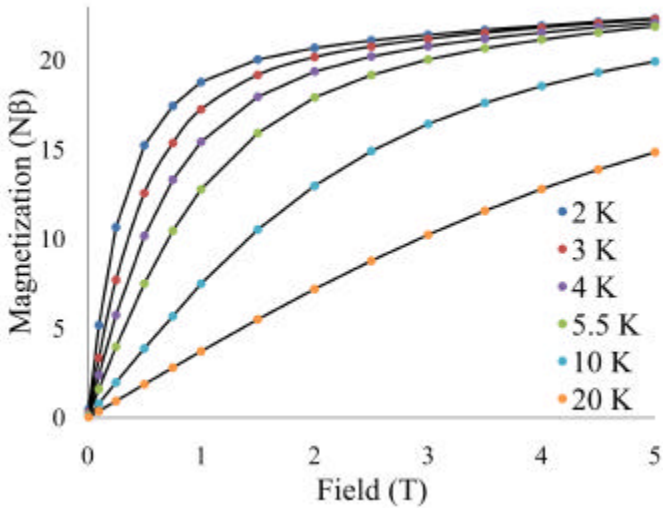

Figure S6. *M* vs *H* isothermal plots for **2** in the 2 (top) – 20 K (bottom) temperature range. The solid lines are guides for the eye.

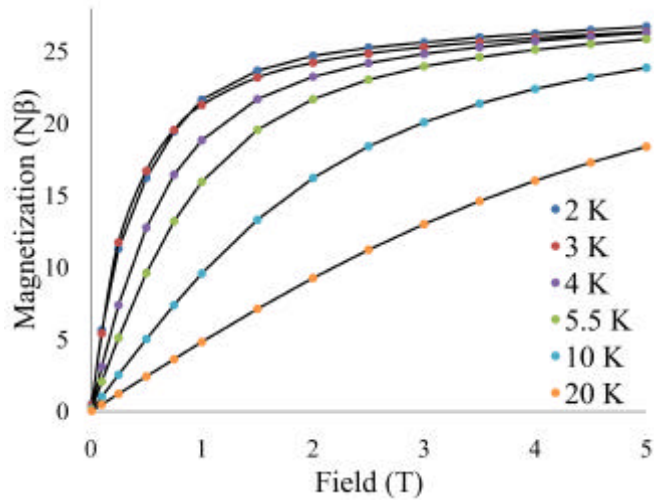

Figure S7. *M* vs *H* isothermal plots for **3** in the 2 (top) – 20 K (bottom) temperature range. The solid lines are guides for the eye.

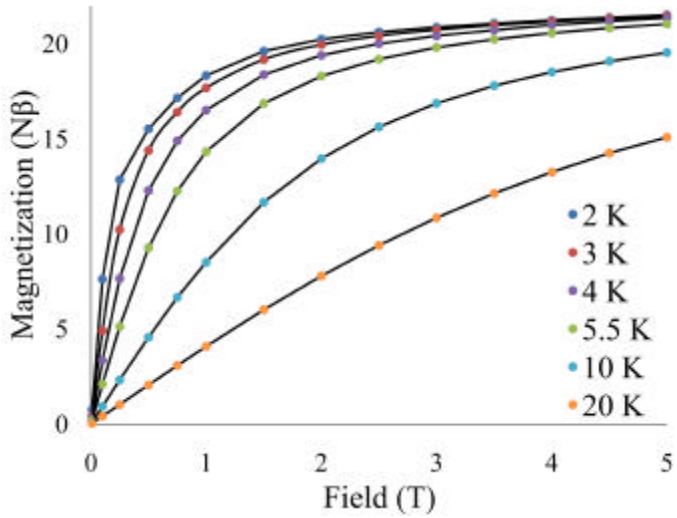

Figure S8. *M* vs *H* isothermal plots for **4** in the 2 (top) – 20 K (bottom) temperature range. The solid lines are guides for the eye.

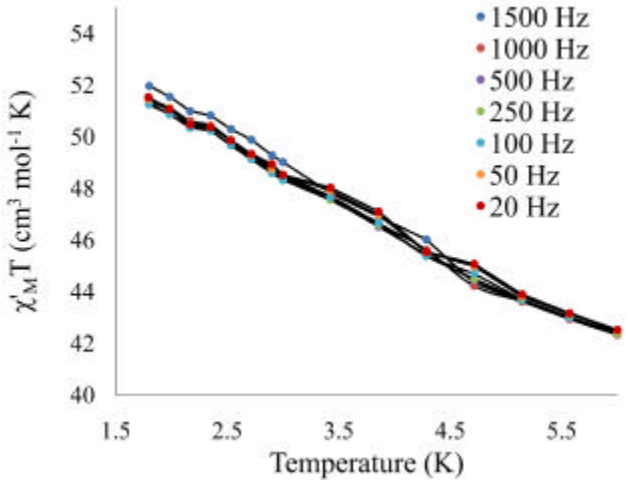

Figure S9. $\chi_M' T$ vs. T for **1**.

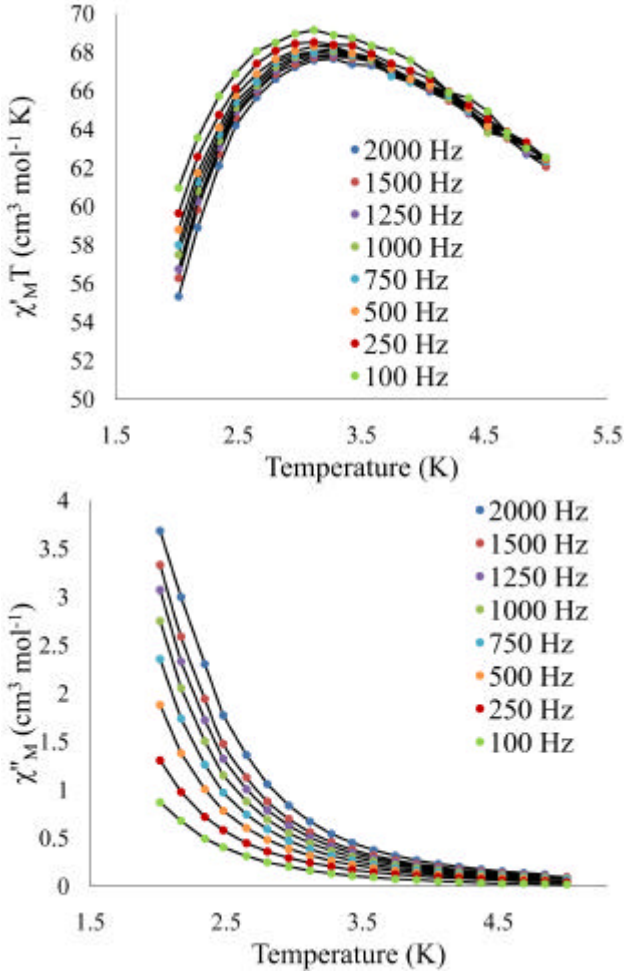

Figure S10. Plots of $\chi_M' T$ vs. T (top) and χ_M'' vs. T for **2** (bottom).

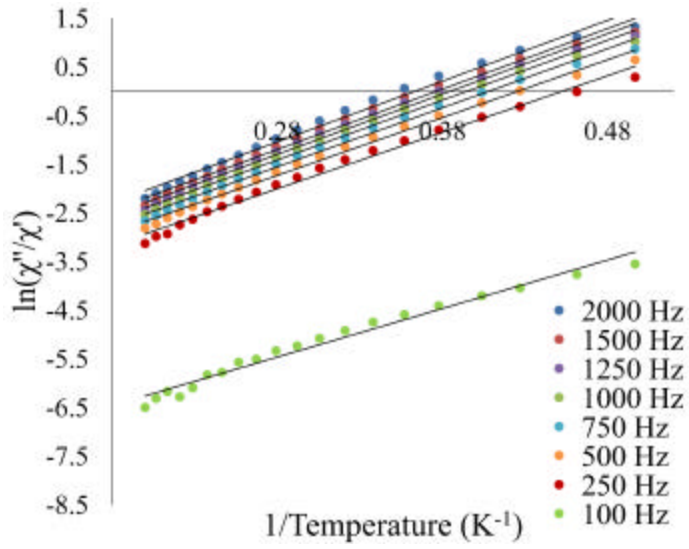

Figure S11. Natural logarithm of the ratio of $?_M''$ over $?_M'$ versus 1/T for **2**.

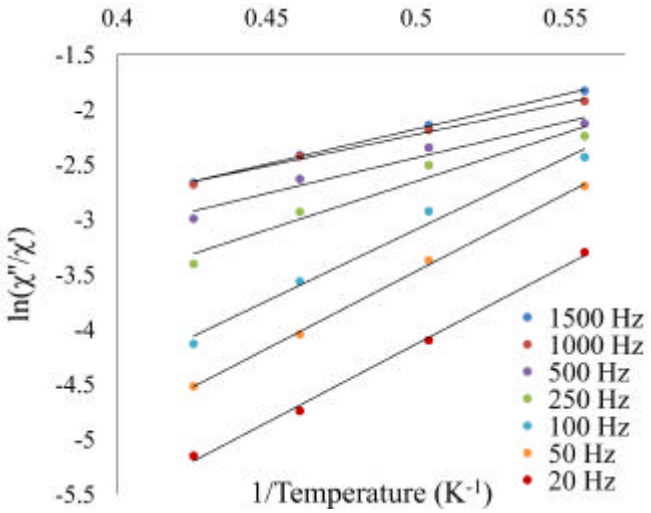

Figure S12. Natural logarithm of the ratio of $?_M''$ over $?_M'$ versus 1/T for **4**.

Computational Details

Details of the computational methods are given in a recent paper and in the supplementary information therein.[1] The magnetic properties of metal centres in the Cu_5Dy_4 complex **3** have been studied by fragment *ab initio* calculations by using a specially designed routine SINGLE_ANISO[2] interfaced with the MOLCAS package.[3] In this connection, suitable mononuclear fragments have to be 'cut' from the molecule, such that this would not change significantly the energy structure on the magnetic centre. To have a good description of the 3d or 4f ligand-field states within a fragment one needs to take into account the influence of the neighbouring metal ions. To this end the neighbouring Dy^{3+} and Cu^{2+} have been simulated by the closed-shell La^{3+} *ab initio* embedding model potentials (AIMP) [4] and Zn2+-AIMP.[4] or by *ab initio* effective core potentials (ECP) of La^{3+} and Sc^{3+}, respectively. The latter approximation is generally expected to be better because the valence electrons of Sc^{3+} and La^{3+} are allowed to hybridize with the ligands' orbitals, which leads to a better description of the charge and covalence effects of the neighbouring Dy^{3+} and Cu^{2+}. The second approximation concerned the coordination sphere. The structures of the calculated fragments are shown in Figures S12 and S14 below. No geometry optimisation on the fragments has been done, all atomic coordinates (except for added hydrogens) being taken from the crystal X-ray analysis. The basis sets used for the calculations were mainly taken from ANO-RCC and ANO-S basis libraries from MOLCAS package.[5]

For the electronic structure, the *ab initio* calculations were performed by means of MOLCAS-7.4 program.[3] The active space for the complete active space self-consisting field (CASSCF) calculation of the dysprosium fragment included the 4f orbitals (CAS (9 in 7)) since we are interested in the ligand field states only. The active space for the CASSCF calculation of the copper fragment included nine electrons in five 3d orbitals. Since the lanthanides have a very strong spin-orbit coupling, a large number of roots should be included in the spin-orbit mixing within the restricted active space state interaction (RASSI-SO) procedure.[6] To avoid convergence problems we had to include in the self-consistent CASSCF calculation all possible roots available for a given active space, but we could mix by spin-orbit interaction only a limited amount of terms. We took in this mixing all roots up to 50000 cm^{-1}. An important aspect of the lanthanide state interaction calculation is that one should take into account all the states coming from an entire multiplet. Taking

fewer roots may induce strong deviations, especially for low-lying multiplets. The number and free ion parentage of states mixed by RASSI are listed together with the fragment description below.

The second order multiconfigurational perturbation calculation (CASPT2) was performed only for the copper fragment. For dysprosium, due to the multitude of states needed to be mixed by spin-orbit coupling, the CASPT2 was too expensive computationally and was not done. With the obtained spin-orbit multiplets, the powder susceptibility and the g-tensors for the lowest Kramers doublets of isolated fragments were further evaluated using the recently developed *ab initio* methodology.[2] The basis of this approach is the *ab initio* calculation of all orbital moment and magnetic moment matrix elements on the relevant spin-orbit multiplets obtained in CASSCF/CASPT2 calculations.[7]

These matrix elements are used in a separate routine to calculate:

(i) magnetic properties measured directly in the experiment (temperature dependent Van Vleck susceptibility tensor and powder averaged function, field-dependent magnetisation for different temperatures and directions and the powder magnetisation). In the present Cu_5Ln_4 study, the calculation of all magnetic properties was done with the same set of exchange coupling parameters given in the text. The diagonalisation of the Zeeman Hamiltonian, written in the basis of 512 exchange eigenfunctions for a particular field strength and direction, yields a set of eigenstates, from which the magnetic moment is computed. The thermally averaged magnetic moment is a Boltzmann-weighted sum of the magnetic moments of different eigenstates at a given temperature. The powder magnetisation, *M*, was obtained by averaging the *M* vectors computed for all orientations of the applied DC field as a function of its strength and temperature.

(ii) parameters of magnetic spin Hamiltonians for different spin-orbit multiplets and groups of spin states, described by the corresponding pseudospin, (*g* tensors, zero-field splitting tensors, etc). In calculations of magnetic properties, all spin-orbit multiplets of ligand-field type on the metal sites are usually taken into account, in particular. This was found to be important for correct quantitative description of the effects of strong magnetic anisotropy and strong applied magnetic fields. Computationally, this routine (SINGLE_ANISO) was interfaced with MOLCAS-7.4 program.

CASSCF / CASPT2 calculations for metal fragments in cluster 3

Dy1 and Dy2 fragments

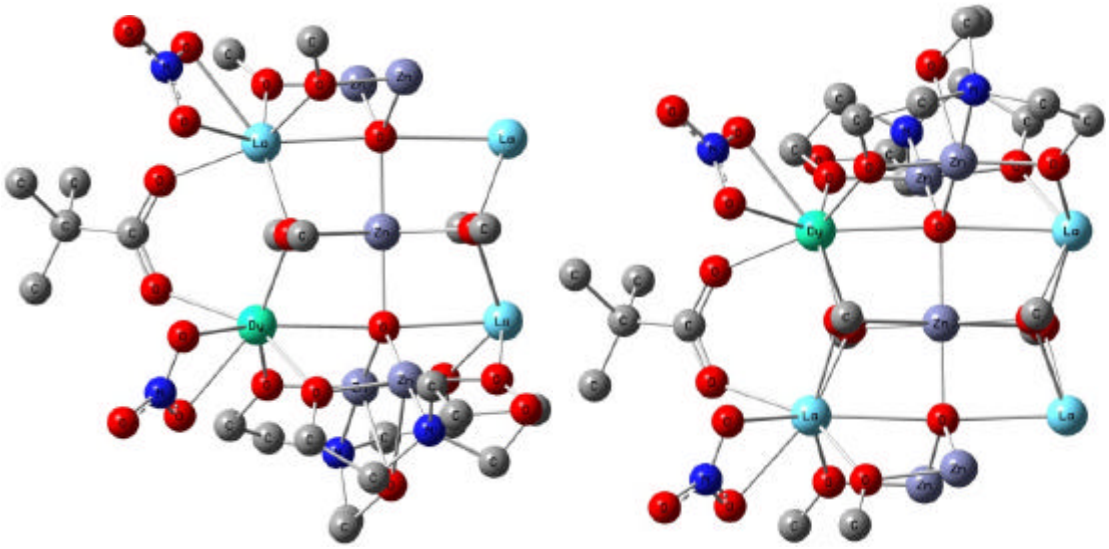

Figure S13. Structure of the calculated Dy1 (right) and Dy2 (left) fragments of the Dy_4Cu_5 complex, **3**. Hydrogen atoms are not shown for clarity.

Basis Sets: All employed basis sets were taken from the standard ANO-RCC basis set library from MOLCAS.[3]

The following contractions were used for the atoms:

Dy – 8s7p5d4f2g1h

La – 7s6p4d3f1g.

Zn – Zn.ECP.Lopez-Moraza.0s.0s.0e-AIMP-KZnF3.

N, O – 4s3p2d. (only for the first coordinated atoms, which make a bond with Dy)

C – 4s3p2d. (only for the atoms that are directly bonded to the first coordination sphere of O and N)

N,O, C – 3s2p. (for distant atoms)

H – 3s1p. (only for the atoms which are directly bonded to the first coordination sphere of O and N)

H – 2s. (for distant atoms)

Active space of the CASSCF method included 9 electrons in 7 orbitals.

The *spin orbit interaction* was computed by mixing of 21 sextets, 128 quartets and 32 doublet spin free states.

Table S1. CASSCF energies of the lowest spin-free states (cm^{-1}) on magnetic sites.

Spin multiplicity		Spin free energies		Spin orbit energies	
		Dy1	Dy2	Dy1	Dy2
6	H	0.000	0.000	0.000	0.000
		11.122	11.316	68.074	70.452
		119.721	109.084	180.233	169.267
		130.541	126.533	247.804	237.840
		307.799	302.647	329.268	338.831
		344.876	341.549	379.097	404.783
		409.526	431.657	452.884	453.878
		443.300	465.087	587.728	531.238
		499.926	511.880	3628.827	3619.931
		680.069	625.366	3678.188	3666.642
		687.904	640.339	3747.281	3753.719
	F	7617.330	7606.854	3783.714	3802.756
		7671.476	7685.155	3845.767	3852.787
		7727.707	7721.720	3928.608	3917.198
		7827.791	7803.085	4023.743	3988.621
		7832.668	7839.958	6202.853	6183.760
		7884.975	7865.861	6255.494	6262.090
		7942.883	7930.267	6291.945	6313.084
	P	34837.747	34794.521	6339.945	6338.954
		34967.159	35032.476	6429.770	6416.407
		35412.486	35365.263	6526.948	6502.613
4		24901.845	24901.666	8159.409	8145.430
		24903.570	24902.341	8216.639	8232.860
		24941.952	24933.944	8255.493	8260.469
		24944.053	24938.516	8355.658	8343.980
		25036.667	25040.671	8449.614	8429.291
		25046.528	25051.868	9695.867	9682.822
		25061.337	25058.261	9754.788	9776.188
		25103.902	25093.789	9851.028	9846.199
		25112.196	25114.186	9974.837	9951.417
		25123.868	25120.462	10068.617	10065.920
		25153.750	25145.740	10105.103	10106.372
		25187.805	25172.308	10136.720	10127.366
		25207.743	25191.904	10172.457	10174.464
		25250.721	25257.225	10245.449	10223.228
		25290.647	25291.508	10279.300	10274.288
		25309.730	25308.795	10882.555	10875.011
		25330.846	25321.372	10997.801	11013.562
		25336.140	25329.171	11217.278	11190.817
		25346.831	25343.444	11601.769	11603.237
		25358.504	25355.513	11635.762	11626.312
		…	…	11662.127	11648.431
2		37354.225	37344.815	11686.860	11680.320
		37355.443	37345.328	11706.699	11701.660

		37370.797	37381.150	13498.500	13495.705
		37371.511	37382.044	13541.926	13532.977
		37460.113	37454.672	13598.053	13589.568
		37468.925	37463.033	13607.236	13601.578
		37504.291	37482.084	14963.963	14960.150
		37524.768	37510.389	15015.546	15006.480
		37577.178	37563.494	15050.816	15044.629
		37585.424	37574.601	15920.835	15916.554
		37607.235	37597.327	15944.325	15935.272
		37609.031	37603.626	16435.279	16428.168
		37622.315	37617.284	25142.668	25139.324
		37658.746	37649.840	25189.341	25169.106
		37666.813	37655.199	25230.812	25238.022
		37676.689	37668.945	25264.203	25270.182
		37687.725	37675.470	25306.943	25311.465
		39024.029	39017.440	25327.060	25324.725
		39025.740	39018.819	25360.707	25356.547
		39047.770	39051.325	25415.125	25418.757
		…	…	…	…

Table S2. Main values of the *g*-tensor for the lowest Kramers doublets on Dy sites.

Kramers doublet		**Main values of the g-tensor**	
		Dy1	**Dy2**
1	g_x	0.0124	0.0116
	g_y	0.0238	0.0247
	g_z	19.6676	19.7190

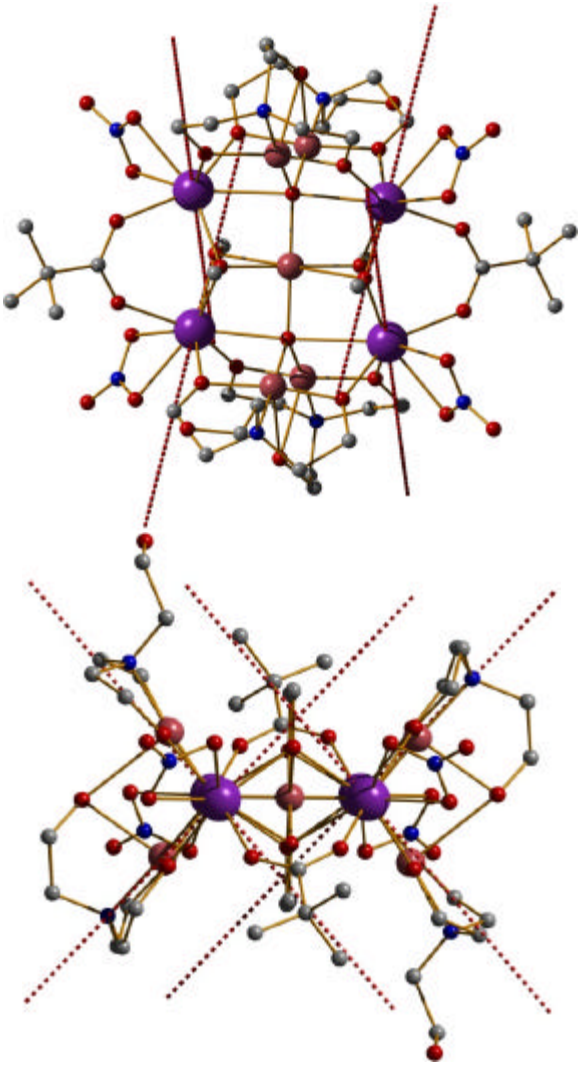

Figure S14. Calculated magnetic axes corresponding to the lowest Kramers doublet on dysprosium sites.

Fragments Cu1m, Cu2m and Cu3c

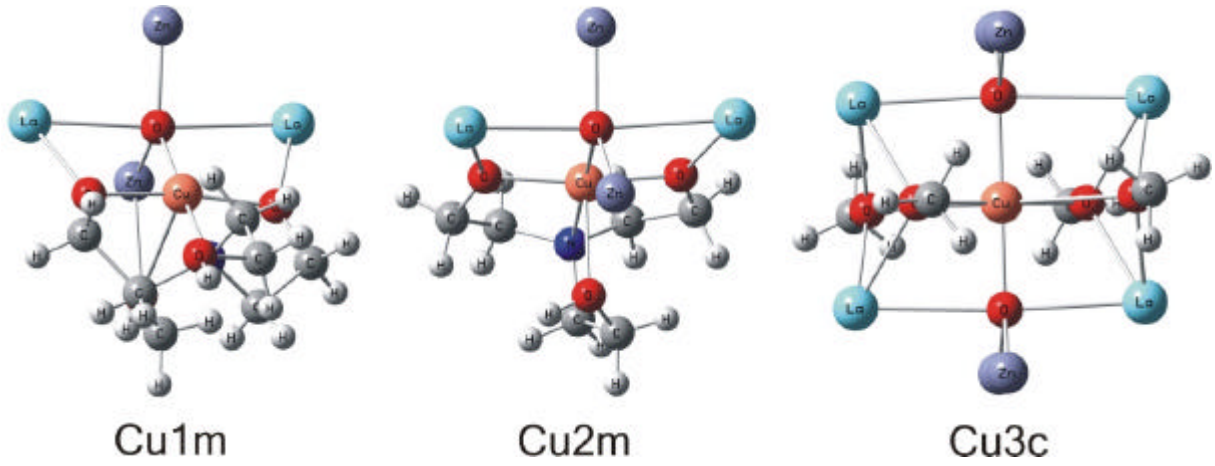

Figure S15. Structure of the calculated copper fragment of the Dy_4Cu_5 complex. Hydrogen atoms are not shown for clarity.

Fragments Cu1m, Cu2m, Cu3c

Basis Sets: All employed basis sets were taken from the standard ANO-RCC basis set library from MOLCAS. The following contractions were used for the atoms:

Cu – 7s6p4d3f2g1h.

La – La.ECP.deGraaf.0s.0s.0e-La(LaMnO3).

Zn – Zn.ECP.Lopez-Moraza.0s.0s.0e-AIMP-KZnF3.

N, O – 4s3p2d1f. (only for the first coordinated atoms, which make a bond with Dy)

C – 4s3p2d. (only for the atoms which are directly bonded to the first coordination sphere of O and N)

N,O, C – 3s2p. (for distant atoms)

H – 3s1p. (only for the atoms which are directly bonded to the first coordination sphere of O and N)

Active space of the CASSCF method included 9 electrons in 10 orbitals.

The *spin orbit interaction* was computed by mixing of 5 doublet spin free states arising from the ^2D multiplet of the Cu^{II} free ion d^9 configuration.

Table S3. Energies of the lowest spin-free states (MS-CASPT2) and of the spin-orbit Kramers doublets on copper (II) sites (cm^{-1}).

Nr.	Spin-free energies			Spin-orbit energies		
	Cu1m	Cu2m	Cu3c	Cu1m	Cu2m	Cu3c
1	0.000	0.000	0.000	0.000	0.000	0.000
2	16124.130	13589.203	10365.722	15883.399	13368.115	10222.520
3	16956.259	15464.613	11882.509	17070.698	15390.644	11877.860
4	18683.463	15548.952	13429.135	18534.048	15815.479	13639.446
5	19722.685	18375.935	15598.027	20296.700	18730.982	15941.222

Table S4. Main values of the *g*-tensor for the lowest Kramers doublets on the three Cu(II) sites.

Kramers doublet		Main values of the g-tensor		
		Cu1m	Cu2m	Cu3c
1	g_x	2.0683	2.0584	2.0341
	g_y	2.0860	2.1222	2.1755
	g_z	2.3518	2.3728	2.4743

Table S5. Exchange energies (cm^{-1}) and main values of the *g*-tensor for the 10 lowest exchange multiplets in **3**.

ID	Energy (cm^{-1})	Multiplicity	Pseudospin	Main values of the g-tensor	
1	0.000000000	2	$\tilde{S}=\frac{1}{2}$	g_x	0.0000
				g_y	0.0000
				g_z	61.0231
2	0.314753081	4	$\tilde{S}=\frac{3}{2}$	g_x	0.0000
				g_y	0.0000
				g_z	29.2488
3	0.380982859	2	$\tilde{S}=\frac{1}{2}$	g_x	0.0000
				g_y	0.0000
				g_z	54.7480
4	0.629506336	2	$\tilde{S}=\frac{1}{2}$	g_x	0.0000
				g_y	0.0000
				g_z	69.7816
5	1.067354680	4	$\tilde{S}=\frac{3}{2}$	g_x	0.0000
				g_y	0.0000
				g_z	26.5115
6	1.180148183	4	$\tilde{S}=\frac{3}{2}$	g_x	0.0000
				g_y	0.0000
				g_z	18.6491
7	1.185438730	4	$\tilde{S}=\frac{3}{2}$	g_x	0.0000

				g_y	0.0000
				g_z	18.6120
8	1.610780386	4	$\tilde{S} = \frac{3}{2}$	g_x	0.0000
				g_y	0.0000
				g_z	20.2658
9	1.616679857	2	$\tilde{S} = \frac{1}{2}$	g_x	0.0000
				g_y	0.0000
				g_z	45.2124
10	1.753731902	4	$\tilde{S} = \frac{3}{2}$	g_x	0.0000
				g_y	10.0707
				g_z	22.5885

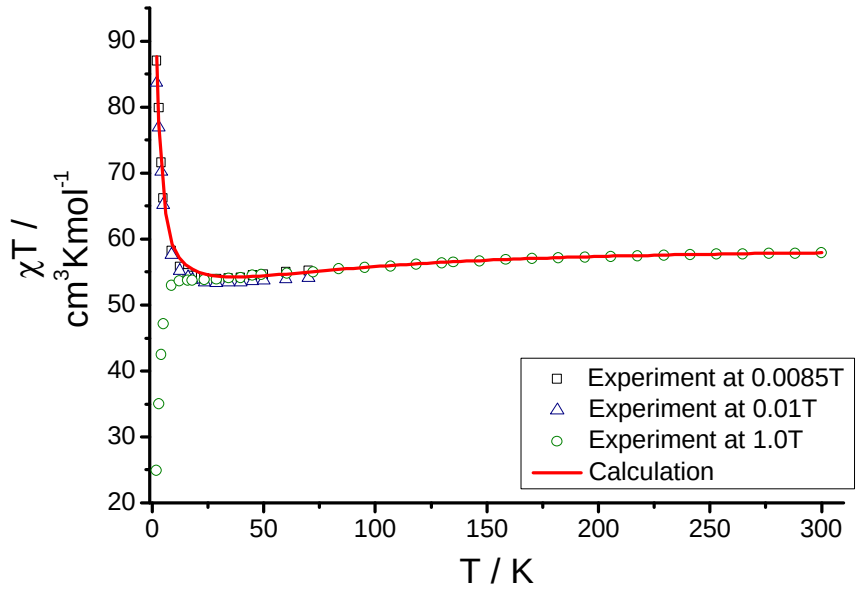

Figure S16. A comparison between measured magnetic susceptibility ($?_M T$) at different applied DC fields and calculated (red line) magnetic susceptibility for the Dy_4Cu_5 complex, **3**.

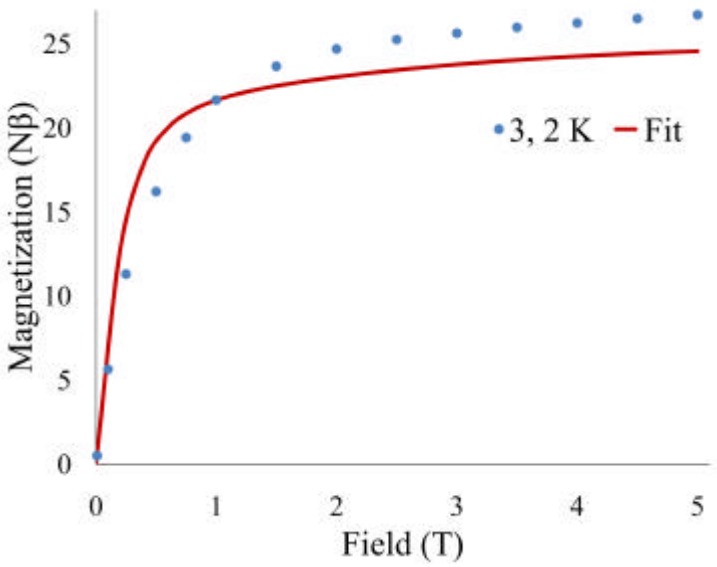

Figure S17. A comparison between measured (blue dots) and calculated (red line) molar magnetization at 2.0 K for the Dy_4Cu_5 complex.

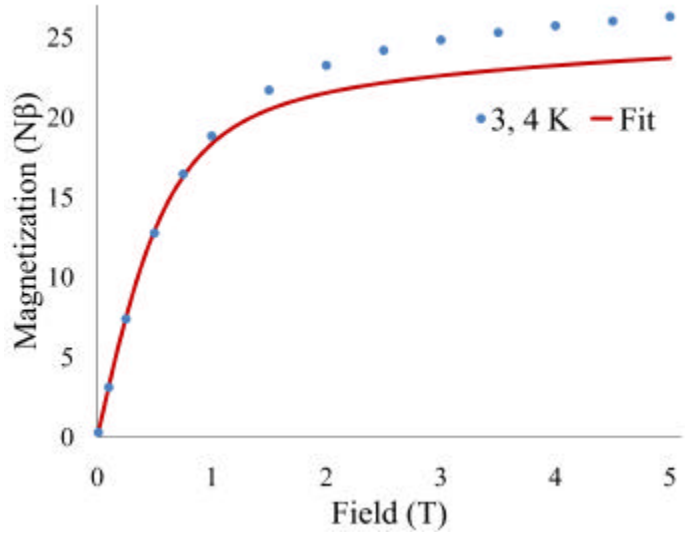

Figure S18. A comparison between measured (blue dots) and calculated (red line) molar magnetization at 4.0 K for the Dy_4Cu_5 complex.

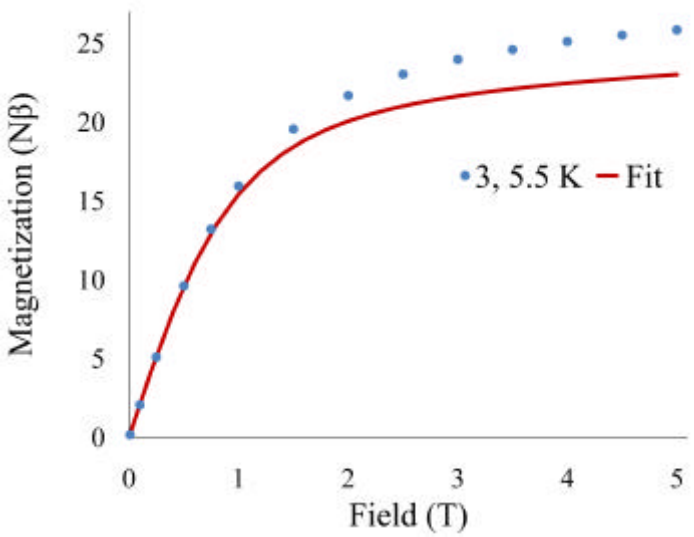

Figure S19. A comparison between measured (blue dots) and calculated (red line) molar magnetization at 5.5 K for the Dy_4Cu_5 complex.

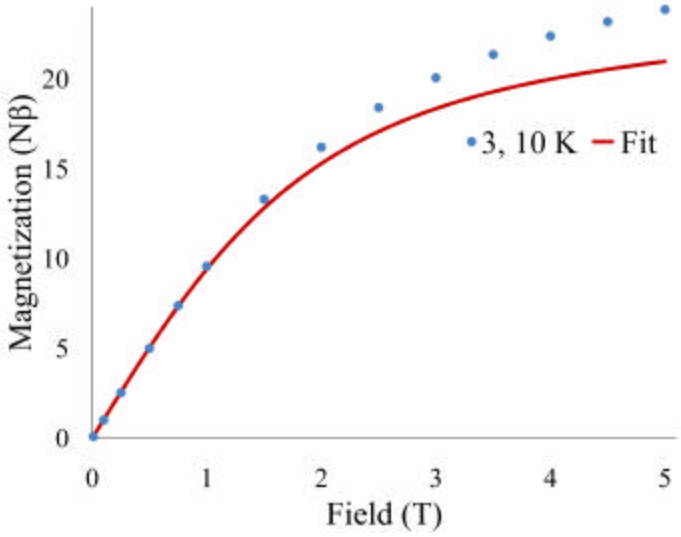

Figure S20. A comparison between measured (blue dots) and calculated (red line) molar magnetization at 10 K for the Dy_4Cu_5 complex.

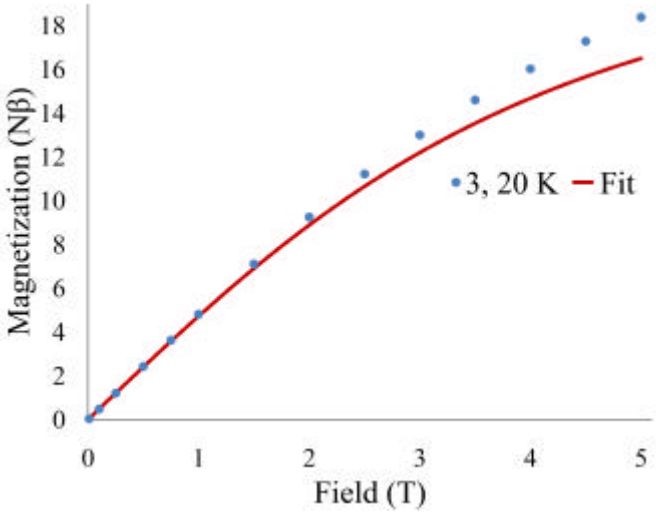

Figure S21. A comparison between measured (blue dots) and calculated (red line) molar magnetization at 20 K for the Dy_4Cu_5 complex.

References

[1] J. Rinck, G. Novitchi, W. Van den Heuvel, L. Ungur, Y. Lan, W.Wernsdorfer, C. E. Anson, L. F. Chibotaru, and A. K. Powell, *Angew. Chem. Int. Ed.* **2010**, 49, 7583-7587.

[2] L. F. Chibotaru, L. Ungur, Program SINGLE_ANISO, University of Leuven 2006.

[3] G. Karlström, R. Lindh, P. -Å. Malmqvist, B. O. Roos, U. Ryde, V. Veryazov, P. -O. Widmark, M. Cossi, B. Schimmelpfennig, P. Neogrady, L. Seijo, *Comp. Mater. Sci.* **2003**, *28*, 222-239.

[4] L. Seijo, Z. Barandiarán, in *Computational Chemistry: Reviews of Current Trends* **1999,** *4*, ed. by J. Leszcynski (World Scientific, Singapore), 55-152.

[5] K. Pierloot, B. Dumez, P.-O. Widmark and B. O. Roos, *Theor. Chim. Acta* **1995**, *90*, 87.; B. O. Roos, R. Lindh, P-O. Malmqvist,V. Veryazov V., P. O. Widmark, *J. Phys. Chem. A*, **2004**, *108*, 2851.

[6] B. O. Roos, P-O. Malmqvist, *Phys. Chem. Chem. Phys.* **2004**, *6*, 2919-2927.

[7] L. Ungur, W. Van den Heuvel, L.F. Chibotaru, *New J. Chem.* **2009**, *33*, 1224-1230.